Vol. 11 (2018) *Acta Physica Polonica B Proceedings Supplement* No 2

DEEP LEARNING APPROACH TO MEASUREMENT OF HIGGS BOSON CP IN THE $H \to \tau\tau$ DECAY CHANNEL*

Elisabetta Barberio[a], Brian Le[a,b], Elzbieta Richter-Was[c]
Zbigniew Was[b,d], Daniele Zanzi[a]

[a]School of Physics, The University of Melbourne
Cnr Swanston St. and Tin Alley, Parkville 3010, Victoria, Australia
[b]H. Niewodniczański Institute of Nuclear Physics, Polish Academy of Sciences
Radzikowskiego 152, 31-342 Kraków, Poland
[c]M. Smoluchowski Institute of Physics, Jagiellonian University
Łojasiewicza 11, 30-348 Kraków, Poland
[d]CERN, PH-TH, 1211 Geneva 23, Switzerland

(Received January 22, 2018)

The measurement of the Higgs boson CP is amongst the most vital measurements in establishing the nature of the Higgs boson. Of the many decay channels, the ditau final state is one of the most sensitive channels due to the Yukawa coupling allowing access to a potential mixing between CP-even and CP-odd Higgs bosons. While decay modes such as the $\tau \to \rho^{\pm}\nu$ are well-established in literature, modes such as the $\tau \to a_1^{\pm}\nu$ are not so. A new approach to encompass many decay modes has been developed using deep learning neural networks. This article summarises work done in assessing the robustness of the approach with respect to detector resolution effects and potential modelling issues. Also discussed is the Drell–Yan background.

DOI:10.5506/APhysPolBSupp.11.349

1. Introduction

The substantial progress of the ATLAS and CMS collaborations since the discovery of the Higgs boson in 2012 has yielded many concise measurements of its properties. The decays of the Higgs boson to dibosons have been discovered and its couplings subsequently well-measured [1]. Evidence for decays to τ leptons and b quarks are now claimed by ATLAS and CMS

* Presented by B. Le with additional material from Zbigniew Was' talk at the Final HiggsTools Meeting, Durham, UK, September 11–15, 2017.

experiments [2–4]. Measurements of the spin-CP, using the dibosonic decays of the Higgs boson, have excluded several alternate hypotheses such as spin 1, spin 2 and pure pseudoscalar (CP-odd, spin-0) cases [5–13]. From current measurements, the couplings of the Higgs boson appear to be fairly consistent with the Standard Model (SM) expectations. Still potential new physics enters measurements of the couplings in more subtle ways.

Several beyond SM (BSM) scenarios predict the existence of a CP-odd Higgs boson. These include Supersymmetry models as well as Two Higgs Doublet models [14–16]. In these scenarios, it is possible for a pseudoscalar Higgs boson to become degenerate with the scalar SM Higgs boson, producing a mixed CP state. While upper limits have been set on anomalous couplings between a pseudoscalar Higgs boson and two gauge bosons in effective field theories, these studies only concern the dibosonic decay modes which are not sensitive to direct couplings to a pseudoscalar Higgs boson [6–8,10,12]. The fermionic decay modes, in which the Yukawa coupling allows direct couplings to pseudoscalar Higgs bosons, are an ideal channel to measure any potential mixings.

Much of the literature proposes the measurement of the CP phase of the Higgs boson in the ditau final state [17–21]. The large branching ratio and relatively clean signal (in comparison to the bb final state) make for a strong candidate for the measurement. Ultimately though, only few of the decay modes of the τ have robust CP sensitive variables constructed (the decays via a ρ resonance remains the the simplest to use despite only consisting 6.5% of the ditau branching ratio). This article outlines a new approach (detailed in [22, 23]) to the construction of CP sensitive observables through the use of deep learning techniques which have been shown to be effective in encapsulating a broader range of decay modes. Furthermore, a discussion of the Z background is also presented.

2. Constructing CP sensitive observables

The means by which a CP sensitive observable can be constructed is detailed well [17–21]. Starting with a Lagrangian

$$\mathcal{L}_{\text{int}} = g_\tau \overline{\tau}(\cos\phi_\tau + \sin\phi_\tau i\gamma_5)\tau h\,, \tag{2.1}$$

where ϕ_τ parameterises the mixing of couplings between CP-even and CP-odd Higgs bosons. Calculating the Higgs boson decay width the sensitivity to the mixing angle is evident with respect to transverse spin components of the outgoing τ leptons

$$\Gamma\left(h_{\text{mix}} \to \tau^+\tau^-\right) \sim 1 - s_{\parallel}^{\tau^+} s_{\parallel}^{\tau^-} + s_{\perp}^{\tau^+} R(2\phi_\tau) s_{\perp}^{\tau^-}\,, \tag{2.2}$$

where R is a rotation in the x–y (transverse) plane [19] and respectively, $s_{\parallel}^{\tau^+}$, $s_{\perp}^{\tau^+}$ are the spin components of the τ which are transverse and parallel to the direction of the τ momenta in the Higgs rest frame. This effect is best observed in the angular distributions of the decay products of the τ lepton.

For τ decays which occur via the chain $\tau^{\pm} \to \rho^{\pm}\nu \to \pi^{\pm}\pi^{0}\nu$, the acoplanarity angle has been shown to be sensitive to the mixing angle [18,19]. For this decay mode, the acoplanarity angle is defined as the angle between the two planes spanned by the visible products of each of the τ. Additionally, another variable y must be defined in order to separate events and give a measureable modulation. This y is defined as

$$y = \frac{E_{\pi^{\pm}} - E_{\pi^{0}}}{E_{\pi^{\pm}} + E_{\pi^{0}}}\,, \tag{2.3}$$

where E is the lab-frame energy of the pions in the decay. This variable is a lab-frame manifestation of the $\cos\theta$ between directions of the pions in the rest frame of the Higgs, which when integrated over cancels any modulation in the acoplanarity angle. Based on the overall sign of the product of the y for each τ events are separated in order to produce a modulation. Owing to the simplicity of the decay, this angle is defined in an unambiguous and fairly robust manner.

For more complex decays, such as those which occur through the chain $\tau^{\pm} \to a_1^{\pm}\nu \to \pi^{\pm}\rho^{0}\nu \to \pi^{\pm}\pi^{\pm}\pi^{\mp}\nu$, it is not as evident how exactly to define the acoplanarity angle in this case. Due to the ambiguity in defining a singular observable, the sensitivity which can be achieved is diluted (see Fig. 1).

The approach of simply taking the acoplanarity angles is not effective for complex decays. In spite of the complexity of the a_1–a_1 decay, the integration of these decays would yield a significant increase in the useable fraction of $H \to \tau\tau$ decays (from 6.5% with only decays via the ρ to 11.9% with the inclusion of a_1 decays). For a_1–a_1 decays though, it is possible to form 16 acoplanarity angles with 8 separating y variables. The multi-dimensionality of the problem indicates a need for a more comprehensive approach. A new approach using neural networks is taken in order to define a new CP sensitive observable. The goal is to globally include as much information as possible about the decay in a manner which can be generalised for even complicated decays such as those involving the a_1 resonance.

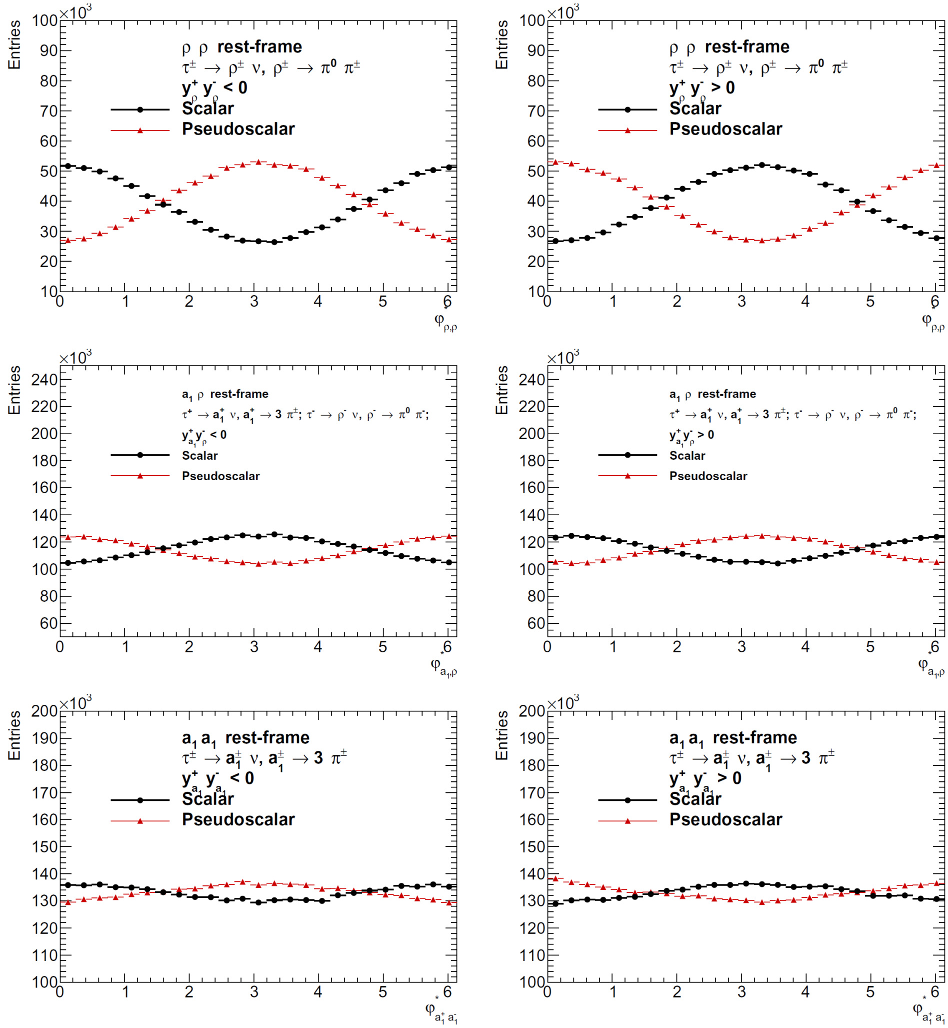

Fig. 1. Acoplanarity angles of $H \to \tau\tau$ decays in the ρ–ρ (top), a_1–ρ (middle) and a_1–a_1 (bottom) decay modes [22]. The more complex decays which involve a_1 resonances have a much smaller separation in the amplitude of the modulation between scalar and pseudoscalar. The a_1–a_1 decays have a $\sim 1\%$ separation in the amplitude compared to $\sim 20\%$ for the simpler ρ–ρ case. Plots right (left) show events where the total product of the y of each τ is greater (less) than zero.

3. Neural network approach

This section summarises work presented in [22, 23]. The inputs, method and results are described.

Monte Carlo (MC) simulation was used to train and test the approach. Between 2 and 5 million $H \to \tau\tau$ events were generated for each decay mode using `Pythia 8.2`. The decays were simulated using the `TAUOLA` library [24] and the `TauSpinner` [25] package was used to calculate the weights for the scalar and pseudoscalar hypotheses. Of these events, after separating events for training and testing as well as application of ATLAS detector acceptance selections for the leptons, approximately 500 000 events were utilised for training the neural networks.

Input features which can potentially demonstrate separation are calculated:

— ϕ^* — The acoplanarity angle, basic CP sensitive variable which is defined as the angle between two planes [18]. All possible combinations between pairs and triplets of pions are accounted for.

— y — The separating variable used to categorise events such that modulations in the acoplanarity angle are evident [18]. The definition for decays to $\rho^\pm$ resonances was detailed in Eq. (2.3). A modification is required for decays of $a_1 \to \rho^0\pi^\pm$ due to the large mass of the ρ^0 resonance. For these decays, y is defined as $\frac{E_{\rho^0}-E_{\pi^\pm}}{E_{\rho^0}+E_{\pi^\pm}} - \frac{m^2_{a_1}-m^2_{\pi^\pm}+m^2_{\rho^0}}{2m^2_{a_1}}$ [22].

— m_i — Invariant masses for pairs or triplets of pions. This is especially useful for a_1 decays, potentially used as a constraint for which pions form the intermediate ρ^0.

— 4-vectors — The four-momenta (calculated in the lab-frame) of the outgoing pions. It was shown in [22] that this class, with some manipulation, can be effectively used as a set of low-level inputs. This class was boosted into the rest frame of the visible decay products and then rotated such that one of the reconstructed taus aligns along the positive z-axis. In principle, this class contains all that is required to reconstruct the other variables mentioned.

With the inputs calculated, neural networks were trained using different combinations of these input variables. The neural networks, consisting of six dense layers of 300 nodes and a single ouput node (the classifier score), were trained on the MC datasets described earlier. A minimal amount of dropout was implemented to prevent overtraining whilst still retaining sensitivity. The networks were trained to separate the scalar and pseudoscalar hypotheses for a given decay mode. The area under the receiver operating characteristic curve (AUC) was taken as the metric for the separation power of each network [26].

4. Potential systematic uncertainties

This section summarises work presented in [23]. The method and results are described.

Before discussing the results of the NN training, considerations of potential systematic uncertainties should be discussed. The limited detector resolution limits the precision in the reconstruction of the four momenta of the outgoing pions, and this may reduce the sensitivity of the NN approach. To address this, simple Gaussian smearings (based on detector resolutions representative of the ATLAS detector [27, 28]) were applied to the MC in order to assess the potential impact.

Additionally, the impact on the NN approach from systematic uncertainties related to the modelling of τ decays is also presented. The factorisation of the τ modelling effects from the Drell–Yan background production is also discussed.

4.1. Detector resolution effects

Training against generator level MC provides a baseline for the sensitivity of the approach, however this does not encapsulate the limitations due to the detector resolution. The degradation due to detector resolution is assessed by smearing original (ideal) MC to produce samples which are more representative of the conditions in the ATLAS detector. Separate NNs are trained on these smeared samples.

Table I (from [23]) presents the AUC score calculated by applying the NN trained on their respective MC (either ideal or smeared) to their respective test dataset for combinations of input features. The quoted statistical and systematic uncertainties are calculated by applying bootstrap and smearing tests on the dataset (described in detail in [23]).

The results from Table I demonstrate only a very small loss in sensitivity ($\sim 1\%$) by training on the smeared samples. This trend is consistent across both decay modes tested and the different combinations of input features indicating the NN approach is robust against smearing.

4.2. Systematic due to τ modelling

One source of systematic uncertainty which could impact the sensitivity of the NN is how the τ decays are modelled. The `TAUOLA` library [24] models the τ decays using data-driven parameterisations using information from low-energy collider experiments such as CLEO [30] and BaBar [31]. Decays via the a_1 resonance may be sensitive to the modelling as spin is propagated to the vector resonances; this is difficult to measure. Thus, through the spin correlations between τ leptons (which is sensitive to the CP of the Higgs boson), the modelling of the decays via the a_1 may be a crucial systematic which affects the NN approach.

TABLE I

AUC scores for NNs trained on various combinations of input features (those used are marked with a ✓) [23]. The columns represent the results for training (and application) on "Ideal" and "Smeared" samples as well as a comparison with [22].

Features				Ideal ± (stat.)	Smeared ± (stat.) ± (syst.)	From [22]
ϕ^*	4-vec	y_i	m_i			
a_1–ρ Decays						
✓	✓	✓	✓	0.6035 ± 0.0005	$0.5923 \pm 0.0005 \pm 0.0002$	0.596
✓	✓	✓	—	0.5965 ± 0.0005	$0.5889 \pm 0.0005 \pm 0.0002$	—
✓	✓	—	✓	0.6037 ± 0.0005	$0.5933 \pm 0.0005 \pm 0.0003$	—
-	✓	—	—	0.5971 ± 0.0005	$0.5892 \pm 0.0005 \pm 0.0002$	0.590
✓	✓	—	—	0.5971 ± 0.0005	$0.5893 \pm 0.0005 \pm 0.0002$	0.594
✓	—	✓	✓	0.5927 ± 0.0005	$0.5847 \pm 0.0005 \pm 0.0002$	0.578
✓	—	✓	—	0.5819 ± 0.0005	$0.5746 \pm 0.0005 \pm 0.0002$	0.569
a_1–a_1 Decays						
✓	✓	✓	✓	0.5669 ± 0.0004	$0.5657 \pm 0.0004 \pm 0.0001$	0.573
✓	✓	✓	—	0.5596 ± 0.0004	$0.5599 \pm 0.0004 \pm 0.0001$	—
✓	✓	—	✓	0.5677 ± 0.0004	$0.5661 \pm 0.0004 \pm 0.0001$	—
—	✓	—	—	0.5654 ± 0.0004	$0.5641 \pm 0.0004 \pm 0.0001$	0.553
✓	✓	—	—	0.5623 ± 0.0004	$0.5615 \pm 0.0004 \pm 0.0001$	0.573
✓	—	✓	✓	0.5469 ± 0.0004	$0.5466 \pm 0.0004 \pm 0.0001$	0.548
✓	—	✓	—	0.5369 ± 0.0004	$0.5374 \pm 0.0004 \pm 0.0001$	0.536

To test this potential effect, various parameterisations of the τ modelling were tested against NNs trained on the default CLEO based hadronic current paramerisation, the default for the `TAUOLA` library. The following variations on the hadronic current modelling are used for testing:

- Standard CLEO (STD) — the default parameterisation [30] based on the Kühn–Santamaria (KS) model [32].
- Alternative CLEO (ALT) — a variation of the STD described in [33] which is taken from an isospin rotation from $\pi^0\pi^0\pi^-$ to the $\pi^-\pi^-\pi^+$ channel.
- BaBar (BBR) — the same KS model as with the STD current but using measurements from the BaBar Collaboration [34].
- Resonance Chiral Lagrangian (RχL) — a fundamentally different model to the KS detailed in [35].

Figures 2, 3 and 4 (from [23]) demonstrate the mass (which typically is used to determine good modelling of the τ decays) and the effect of the different parameterisations on the acoplanarity angle (the baseline CP sensitive observable). Despite the acoplanarity showing little significant variation, it is important that the correlations be checked in the NN.

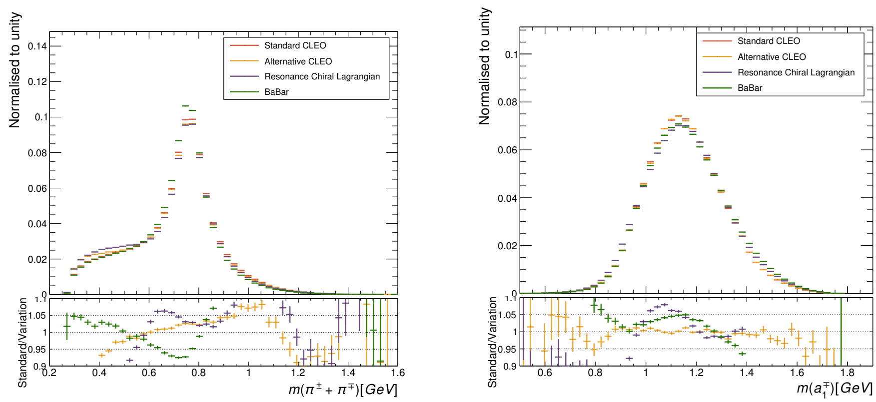

Fig. 2. Invariant masses constructed from $\tau^{\mp} \to a_1^{\mp}\nu \to 3\pi^{\mp}\nu$ decays [23]. Ratios between the alternative parameterisation (RχL, ALT, BBR) and the baseline (STD) parameterisation are given in the lower panels. The mass from summing two oppositely charged pions and three pions from the a_1 decay are shown on the left and right plots respectively.

In order to check if the variations cause a loss in sensitivity, NNs which were trained on MC generated with the standard CLEO parameterisation are applied to MC generated with the other three variations.

The results in Table II (from [23]) show that the fluctuations in the AUC score (and hence the sensitivity) are within two or three times the quoted statistical uncertainty from Table I. Ultimately, the loss in sensitivity due to training on more detector realistic samples impacts the deep learning approach to a greater degree than the modelling of the τ decay.

4.3. On systematic errors

So far, we have concentrated on the $H \to \tau\tau$ signature and found that even in the case where detector smearing is included, sensitivity can still clearly be obtained, even for the a_1–a_1 decay mode. Modelling of τ decays was also found to be unproblematic.

A good reason why this was the case was because Higgs boson production and decay are well-separated from a physics point of view. This is because the Higgs boson has a narrow width and a spin of zero.

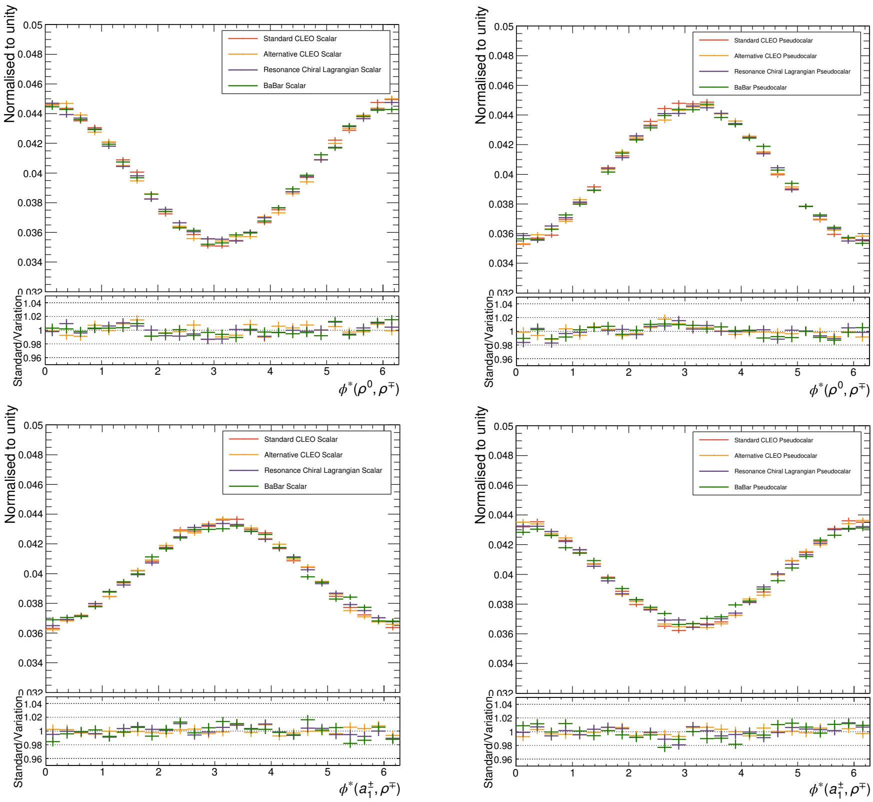

Fig. 3. A comparison of acoplanarity angles calculated for $H \to \tau\tau \to \rho^\mp \nu \; a_1^\pm \nu$ using different parameterisations (STD, RχL, ALT, BBR) for events with $y_1 \cdot y_2 > 0$. Ratios between the alternative parameterisation (RχL, ALT, BBR) and the baseline (STD) parameterisation are given in the lower panels. The rows (top to bottom) contain acoplanarities reconstructed with combinations of 2π–2π, $\rho^0\pi^\pm$–2π, respectively. Each row contains the distributions of the acoplanarity angle for scalar (left) and pseudoscalar (right) hypotheses [23].

The situation of the background is potentially worse. Even though the process can be simulated and transverse spin effects introduced with the help of the spin weights (exactly as in the case of the signal assumption [25]), the separation of Z production and decay is far less established. This could be worrisome, dynamics of jets in the Drell–Yan processes can be a problem as its modelling does not always match well the data [36]. If this effect is intertwined with spin phenomena, this could be problematic.

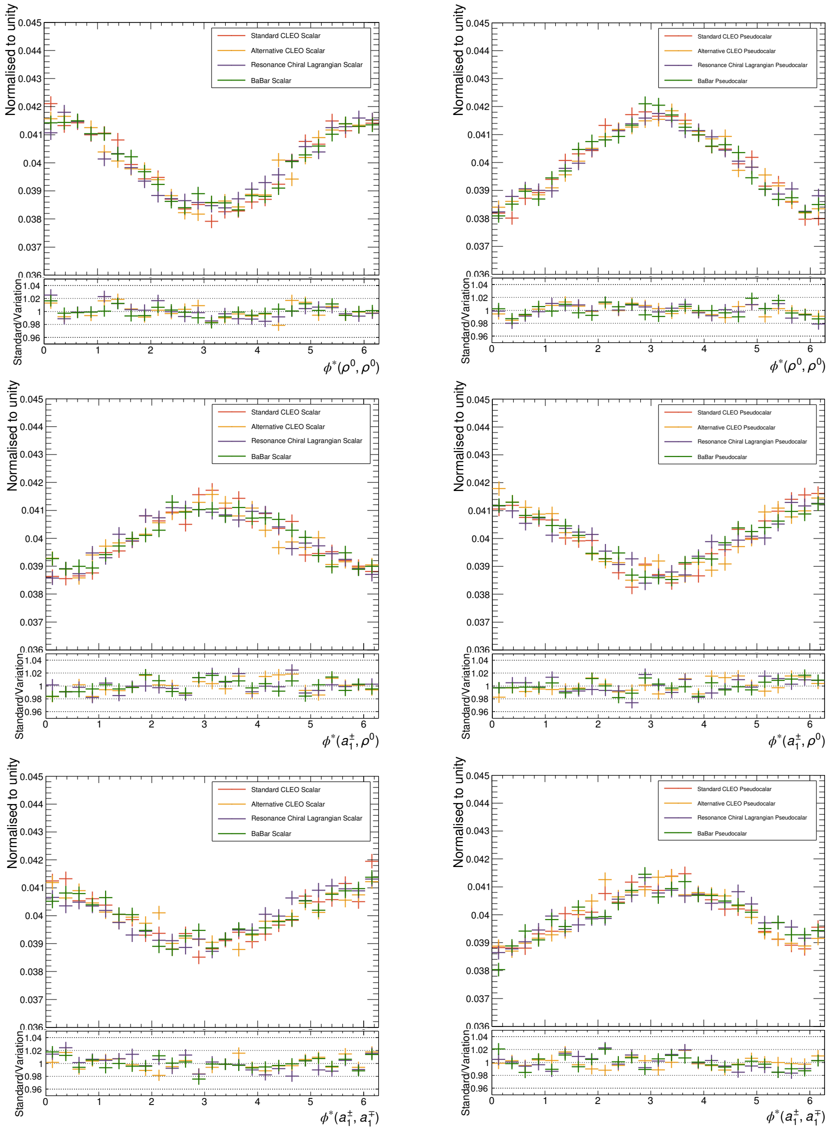

Fig. 4. A comparison of acoplanarity angles calculated for $H \to \tau\tau \to a_1^{\mp}\nu\; a_1^{\pm}\nu$ using different parameterisations (STD, RχL, ALT, BBR) for events with $y_1 \cdot y_2 > 0$. Ratios between the alternative parameterisation (RχL, ALT, BBR) and the baseline (STD) parameterisation are given in the lower panels. The rows (top to bottom) contain acoplanarities reconstructed with combinations of 2π–2π, $\rho^0\pi^{\pm}$–2π, and $\rho^0\pi^{\pm}$–$\rho^0\pi^{\pm}$, respectively. Each row contains the distributions of the acoplanarity angle for scalar (left) and pseudoscalar (right) hypotheses [23].

TABLE II

AUC score for NNs trained with a_1–ρ and a_1–a_1 decays of $\tau\tau$ system using events modelled with the STD and then tested on events generated with alternative parameterisations. The test was performed on ideal MC [23].

Features				STD	RχL	ALT	BBR
ϕ^*	4-vec	y_i	m_i				
				a_1–ρ Decays			
✓	✓	✓	✓	0.604	0.604	0.603	0.603
✓	✓	✓	—	0.597	0.596	0.596	0.597
✓	✓	—	✓	0.604	0.604	0.604	0.604
—	✓	—	—	0.597	0.596	0.596	0.595
✓	✓	—	—	0.597	0.596	0.596	0.595
✓	—	✓	✓	0.593	0.593	0.593	0.593
✓	—	✓	—	0.582	0.579	0.580	0.578
				a_1–a_1 Decays			
✓	✓	✓	✓	0.567	0.563	0.564	0.564
✓	✓	✓	—	0.560	0.555	0.557	0.556
✓	✓	—	✓	0.568	0.564	0.566	0.566
—	✓	—	—	0.562	0.557	0.559	0.559
✓	✓	—	—	0.562	0.557	0.559	0.559
✓	—	✓	✓	0.547	0.546	0.547	0.545
✓	—	✓	—	0.537	0.534	0.535	0.533

The purpose of [37, 38] was different, but the results demonstrate that leptonic final-state dynamic separates well from the production. For the process of $q\bar{q} \to Z/\gamma^* \to l^+l^-$, in which jets are present, the differential cross section can be expressed as

$$\begin{aligned}\frac{\mathrm{d}\sigma}{\mathrm{d}p_{\mathrm{T}}^2\mathrm{d}Y\mathrm{d}\cos\theta d\phi} &= \frac{3}{16\pi}\frac{\mathrm{d}\sigma^{U+L}}{\mathrm{d}p_{\mathrm{T}}^2\mathrm{d}Y} \\ &\times\Big[\left(1+\cos^2\theta\right)+\frac{1}{2}A_0\left(1-3\cos^2\theta\right)+A_1\sin\left(2\theta\right)\cos\phi \\ &+\frac{1}{2}\,A_2\sin^2\theta\cos\left(2\phi\right)+A_3\sin\theta\cos\phi+A_4\cos\theta \\ &+A_5\sin^2\theta\sin\left(2\phi\right)+A_6\sin\left(2\theta\right)\sin\phi+A_7\sin\theta\ \sin\phi\Big]\,, \end{aligned} \tag{4.1}$$

where p_{T} and Y are the transverse momentum and rapidity of the lepton pair, θ and ϕ being the polar and azimuthal angle of the lepton in the dilepton rest frame and $\mathrm{d}\sigma^{U+L}$ is the unpolarised differential cross section. This is true up to corrections of the order of $\alpha_{\mathrm{S}}^2 \sim 0.01$ [39, 40]. The A_i coefficients encode the dynamics of the production process.

The Born-like shapes of cross sections may be preserved, despite the presence of hard, high p_{T} jets. Spherical harmonics with a proper choice of frame (`Mustraal` frames [45]), inspired by studying the first order matrix element, helps to reduce the lepton distribution in lepton-pair frame to essentially a single non-trivial coefficient (all but A_4 — see Fig 5).

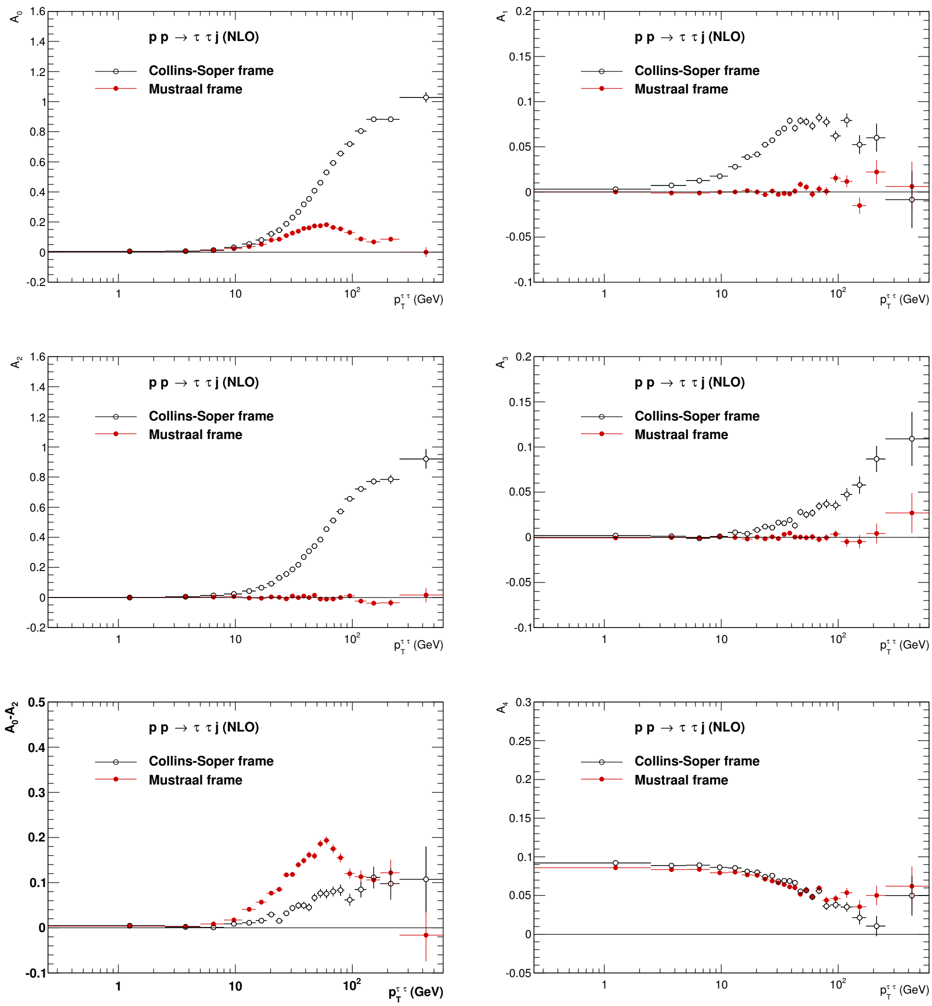

Fig. 5. The A_i coefficients of Eq. (4.1) in Collins–Soper (open symbols/black) and in `Mustraal` (full symbols/red) frames for $pp(q\bar{q}) \to \tau\tau j$ process generated with `Powheg+MiNLO` [41–43]. All but A_4 are shown to be trivial using the `Mustraal` frame.

This is important because the machine learning methodology exposes details of predictions which may be badly modelled in the hadronic sector. One can rely on leptonic variables only; τ-decay products. Everything related to intermediate Z/γ^* production can be kept aside. That is the message one can deduce from references [37, 38].

Finally, let us point that such factorization or semi-factorization was necessary to develop the code of `TauSpinner`, and for discussion of the reliability of its recent extension presented in [44] and in the contributions of proceedings.

5. Conclusion

The measurement of the Higgs boson CP using $H \to \tau\tau$ will be an important measurement in establishing the nature of the Higgs boson. A new deep learning approach has been established to try and create a CP sensitive observable which has the potential of encompassing multiple decay modes. This method has been shown to be robust against detector resolution effects and variations in the τ-decay modelling. The approach will be applicable when considering the dominant Drell–Yan background owing to the results discussed in Section 4.3.

We would like to thank R. Jozefowicz of Open AI (CA USA) for discussions and suggestions concerning NN applications. The authors would like to thank for the support from funding agencies. Brian Le was supported by the Australian Government Research Training Program Scholarship. Brian Le and Zbigniew Was were supported by the European Union under the Grant Agreement PITNGA2012316704 (HiggsTools). Elisabetta Barberio and Daniele Zanzi are supported by the Australian Research Council through the Centre of Excellence for Particle Physics at the Terascale. Zbigniew Was and Elzbieta Richter-Was were supported by the National Science Centre, Poland (NCN) under decisions UMO-2014/15/B/ST2/00049. Part of the simulations were performed at PLGrid Infrastructure of the Academic Computer Centre CYFRONET AGH in Kraków, Poland.

REFERENCES

[1] G. Aad *et al.* [ATLAS, CMS collaborations], *J. High Energy Phys.* **1608**, 045 (2016) [`arXiv:1606.02266 [hep-ex]`].

[2] M. Aaboud *et al.* [ATLAS Collaboration], *J. High Energy Phys.* **1712**, 024 (2017) [`arXiv:1708.03299 [hep-ex]`].

[3] G. Aad *et al.* [ATLAS Collaboration], *J. High Energy Phys.* **1504**, 117 (2015) [arXiv:1501.04943 [hep-ex]].

[4] A.M. Sirunyan *et al.* [CMS Collaboration], *Phys. Lett. B* **779**, 283 (2018) [arXiv:1708.00373 [hep-ex]].

[5] G. Aad *et al.* [ATLAS Collaboration], *Phys. Lett. B* **726**, 120 (2013) [arXiv:1307.1432 [hep-ex]].

[6] V. Khachatryan *et al.* [CMS Collaboration], *Phys. Rev. D* **92**, 012004 (2015) [arXiv:1411.3441 [hep-ex]].

[7] S. Chatrchyan *et al.* [CMS Collaboration], *Phys. Rev. D* **89**, 092007 (2014) [arXiv:1312.5353 [hep-ex]].

[8] V. Khachatryan *et al.* [CMS Collaboration], *Phys. Rev. D* **92**, 072010 (2015) [arXiv:1507.06656 [hep-ex]].

[9] G. Aad *et al.* [ATLAS Collaboration], *Eur. Phys. J. C* **75**, 476 (2015) [*Erratum ibid.* **76**, 152 (2016)] [arXiv:1506.05669 [hep-ex]].

[10] V. Khachatryan *et al.* [CMS Collaboration], *Phys. Lett. B* **759**, 672 (2016) [arXiv:1602.04305 [hep-ex]].

[11] G. Aad *et al.* [ATLAS Collaboration], *Phys. Lett. B* **753**, 69 (2016) [arXiv:1508.02507 [hep-ex]].

[12] A.M. Sirunyan *et al.* [CMS Collaboration], *Phys. Lett. B* **775**, 1 (2017) [arXiv:1707.00541 [hep-ex]].

[13] S. Chatrchyan *et al.* [CMS Collaboration], *Phys. Rev. Lett.* **110**, 081803 (2013) [arXiv:1212.6639 [hep-ex]].

[14] A. Djouadi, *Phys. Rep.* **457**, 1 (2008) [arXiv:hep-ph/0503172].

[15] A. Djouadi, *Phys. Rep.* **459**, 1 (2008) [arXiv:hep-ph/0503173].

[16] E. Accomando *et al.*, arXiv:hep-ph/0608079.

[17] M. Kramer, J.H. Kuhn, M.L. Stong, P.M. Zerwas, *Z. Phys. C* **64**, 21 (1994) [arXiv:hep-ph/9404280].

[18] G.R. Bower, T. Pierzchala, Z. Was, M. Worek, *Phys. Lett. B* **543**, 227 (2002) [arXiv:hep-ph/0204292].

[19] K. Desch, A. Imhof, Z. Was, M. Worek, *Phys. Lett. B* **579**, 157 (2004) [arXiv:hep-ph/0307331].

[20] A. Rouge, *Phys. Lett. B* **619**, 43 (2005) [arXiv:hep-ex/0505014].

[21] S. Berge, W. Bernreuther, S. Kirchner, *Phys. Rev. D* **92**, 096012 (2015) [arXiv:1510.03850 [hep-ph]].

[22] R. Jozefowicz, E. Richter-Was, Z. Was, *Phys. Rev. D* **94**, 093001 (2016) [arXiv:1608.02609 [hep-ph]].

[23] E. Barberio *et al.*, *Phys. Rev. D* **96**, 073002 (2017) [arXiv:1706.07983 [hep-ph]].

[24] N. Davidson *et al.*, *Comput. Phys. Commun.* **183**, 821 (2012) [arXiv:1002.0543 [hep-ph]].

[25] T. Przedzinski, E. Richter-Was, Z. Was, *Eur. Phys. J. C* **74**, 3177 (2014) [arXiv:1406.1647 [hep-ph]].

[26] S.A.G. Arnaud, L. Dominique, http://mlwiki.org/index.php/ROC_Analysis

[27] G. Aad *et al.* [ATLAS Collaboration], *Eur. Phys. J. C* **70**, 787 (2010) [arXiv:1004.5293 [physics.ins-det]].

[28] G. Aad *et al.* [ATLAS Collaboration], *Eur. Phys. J. C* **76**, 295 (2016) [arXiv:1512.05955 [hep-ex]].

[29] B. Efron, *The Jackknife, the Bootstrap and Other Resampling Plans*, Society for Industrial and Applied Mathematics, 1982, DOI:10.1137/1.9781611970319.

[30] D. Asner *et al.* [CLEO Collaboration], *Phys. Rev. D* **61**, 012002 (2000) [arXiv:hep-ex/9902022].

[31] M. Chrzaszcz, T. Przedzinski, Z. Was, J. Zaremba, arXiv:1609.04617 [hep-ph].

[32] J.H. Kühn, A. Santamaria, *Z. Phys. C* **48**, 445 (1990).

[33] J.W. Hinson, Axial Vector and Pseudoscalar Hadronic Structure in $\tau \to \pi^-\pi^-\pi^+\nu_\tau$ Decays with Implications on Light Quark Masses, Ph.D. Thesis, Purdue Universty, 2001.

[34] I.M. Nugent, Precision Measurements of Tau Lepton Decays, SLAC-R-936, Ph.D. Thesis.

[35] D.G. Dumm, P. Roig, A. Pich, J. Portolés, *Phys. Lett. B* **685**, 158 (2010) [arXiv:0911.4436 [hep-ph]].

[36] G. Aad *et al.* [ATLAS Collaboration], *Eur. Phys. J. C* **76**, 322 (2016) [arXiv:1602.00988 [hep-ex]].

[37] E. Richter-Was, Z. Was, *Eur. Phys. J. C* **76**, 473 (2016) [arXiv:1605.05450 [hep-ph]].

[38] E. Richter-Was, Z. Was, *Eur. Phys. J. C* **77**, 111 (2017) [arXiv:1609.02536 [hep-ph]].

[39] R. Kleiss, *Nucl. Phys. B* **347**, 67 (1990).

[40] E. Mirkes, J. Ohnemus, *Phys. Rev. D* **51**, 4891 (1995) [arXiv:hep-ph/9412289].

[41] S. Alioli, P. Nason, C. Oleari, E. Re, *J. High Energy Phys.* **1006**, 043 (2010) [arXiv:1002.2581 [hep-ph]].

[42] P. Nason, *J. High Energy Phys.* **0411**, 040 (2004) [arXiv:hep-ph/0409146].

[43] K. Hamilton, P. Nason, G. Zanderighi, *J. High Energy Phys.* **1210**, 155 (2012) [arXiv:1206.3572 [hep-ph]].

[44] M. Bahmani *et al.*, *Eur. Phys. J. C* **78**, 10 (2018) [arXiv:1708.03671 [hep-ph]].

[45] S. Jadach, B.F.L. Ward, Z. Wąs, *Comput. Phys. Commun.* **79**, 503 (1994).